ELECTROMAGNETIC SCATTERING BY A PERIODIC ARRAY OF CYLINDRICAL OBJECTS EMBEDDED IN A DIELECTRIC SLAB

Kiyotoshi YASUMOTO, Taras KUSHTA, and Kuniaki YOSHITOMI
Department of Computer Science and Communication Engineering
Kyushu University 36, Fukuoka 812-8581, Japan
E-mail yasumoto@csce.kyushu-u.ac.jp

1. INTRODUCTION

Considerable efforts has been invested over the years on the study of electromagnetic scattering from periodic dielectric or metallic strucures. The continuing interest is in their use for frequency selective or polarization selective components in microwaves and optical waves. Recently photonic bandgap structures [1] of discrete periodic dielectric systems have received a growing attention, because they have many potential applications to narrow-band filters, high-quality resonant cavities, and substrates for antennas. A periodic array of cylindrical objects is a two-dimensional discrete periodic structure. The frequency response of a free-standing periodic array is characterized by the scattering properties of the individual cylinders and the multiple scattering effects peculiar to the periodic arrangement of scatterers. When the array is embedded in a dielectric slab, another important effect is incorporated. This is a multiple scattering of fields between the array plane and the slab boundaries. The frequency response of the embedded array might be controlled by varying the slab thickness and material combination. Various analytical or numerical approaches [2]-[4] have been developed to characterize the electromagnetic scattering from the free-standing or embedded periodic arrays.

In this paper, we shall present an accurate and efficient method to analyze electromagnetic scattering from a periodic array of cylindrical objects embedded in a dielectric slab, using the lattice sums formula [5] and the T-matrix for the isolated single cylinder. The method is quite general and applies to a variety of configurations of two-dimensional periodic arrays. The array element can contain two or more cylinders within a unit cell, which may be dielectric, conductor, gyrotropic medium, or their mixture with different sizes. First, the reflection and transmission matrices for the free-standing periodic array are discussed. The results are used to derive the generalized reflection and transmission matrices for the embedded array, which enable us to calculate the reflection and transmission properties. Numerical results of the frequency selective reflection properties are discussed for the array of circular cylinders of dielectric, conductor, and magnetized ferrite.

2. FORMULATION

The goemetry considered here is shown in Fig. 1. A periodic array of cylinders sapaced h units along the x axis is embedded in a dielectric slab of thickness $d = d_1 + d_2$. The permettivities and permeabilities of the cylinders, slab, and background medium are denoted by (ε_g, μ_g), (ε_s, μ_s), and (ε_0, μ_0), respectively. The upper and lower boundaries of the slab are located at $y = d_1$ and $y = -d_2$. We consider the two-dimensional scattering problem of a plane wave impinging on the slab at angle ϕ_0 with respect to the positive x axis.

Let $k_{x0} = k_0 \cos\phi_0$ be the x component of wavevector of the original plane wave impinging on the slab at an angle ϕ_0, and $k_{xl} = k_0 \cos\phi_0 + 2l\pi/h$ be that of the l-th space-harmonic, where $k_0 = \omega\sqrt{\varepsilon_0\mu_0}$. The set of space-harmonics originated from the periodic array is reflected at the upper and lower boundaries of the slab, impinges on the array plane as a set of new incident field, and is scattered again by the array. A series of this process explains a multiple scattering of wave fields between the periodic array and the boundaries of the slab. Such a multiple scattering phenomena can be described in terms of the reflection and transmission matrices of the array plane. Following the same analytical procedure as given in [6], the reflection matrix $\boldsymbol{R}^+$ and the transmission matrix $\boldsymbol{F}^+$ for the downgoing incident waves are deduced as follows:

$$\boldsymbol{R}^+ = \boldsymbol{U}\boldsymbol{P}^s, \quad \boldsymbol{F}^+ = \boldsymbol{I} + \boldsymbol{V}\boldsymbol{P}^s \tag{1}$$

with

$$\boldsymbol{U} = [u_{lm}] = [\frac{2(-i)^m}{k_s h \sin\phi_l} e^{im\phi_l}], \quad \boldsymbol{V} = [v_{lm}] = [\frac{2(-i)^m}{k_s h \sin\phi_l} e^{-im\phi_l}] \tag{2}$$

$$\cos\phi_l = \frac{k_0}{k_s}\cos\phi_0 + \frac{2l\pi}{k_s h}, \quad \sin\phi_l = \left[\begin{array}{ll} \sqrt{1-\cos^2\phi_l} & (\cos^2\phi_l \le 1) \\ i\sqrt{\cos^2\phi_l - 1} & (\cos^2\phi_l > 1) \end{array}\right. \tag{3}$$

$$\boldsymbol{P}^s = (\boldsymbol{I} - \boldsymbol{T}\boldsymbol{L})^{-1}\boldsymbol{T}\boldsymbol{P}^i, \quad \boldsymbol{P}^i = [p_{mn}] = [i^m e^{im\phi_n}] \quad (l, m, n = 0, \pm1, \pm2, \cdots) \tag{4}$$

where δ_{lm} is the Kronecker's delta, $\boldsymbol{I}$ is the unit matrix, and p_{mn} denotes the m-th component of amplitude vector of the downgoing incident n-th space-harmonic in the cylindrical coordinate system. In Eq.(4), $\boldsymbol{T}$ is the T-matrix of the isolated single cylinder and $\boldsymbol{L}$ is a square matrix whose elements L_{mn} are given by the lattice sum $S_{m-n}(k_0 h, \cos\phi_0)$ [5] of (m-n)-th order. Similarly, the reflection matrix $\boldsymbol{R}^-$ and the transmission matrix $\boldsymbol{F}^-$ for the upgoing incident waves are derived as follows:

$$\boldsymbol{R}^- = \boldsymbol{V}\boldsymbol{Q}^s, \quad \boldsymbol{F}^- = \boldsymbol{I} + \boldsymbol{U}\boldsymbol{Q}^s \tag{5}$$

with

$$\boldsymbol{Q}^s = (\boldsymbol{I} - \boldsymbol{T}\boldsymbol{L})^{-1}\boldsymbol{T}\boldsymbol{Q}^i, \quad \boldsymbol{Q}^i = [q_{mn}] = [i^m e^{-im\phi_n}]. \tag{6}$$

where q_{mn} denotes the m-th component of amplitude vector of the upgoing incident n-th space-harmonic in the cylindrical coordinate system. It is easy to show that $\boldsymbol{R}^+ = \boldsymbol{R}^-$ and $\boldsymbol{F}^+ = \boldsymbol{F}^-$ when the cross sectional configuration of cylinders situated in the unit cell is symmetric with respect to the array plane $x = 0$. Note that the lattice sum $S_{m-n}(k_0 h, \cos\phi_0)$ characterizes [5] uniquely the periodic arrangement of scatterers and is independent of the polarization of the incident field and the individual configuration of cylindrical objects. The matrix $\boldsymbol{L}$ calculated once can be commonly used for TE and TM waves and for any arrays of cylindrical objects whenever the periods are same. The details of scattering from each array element are described by the T-matrix $\boldsymbol{T}$ in Eq.(4). We may use an aggregate T-matrix [6] of composite cylinders system when the array contains two or more cylinders within a unit cell.

Now we consider the periodic array embedded in a dielectric slab as shown in Fig. 1. The whole space is separated into four regions. When a plane wave impinges on the slab from the semi-infinite region $y > d_1$, the space harmonic fields in the respective regions are expressed as follows:

$$\boldsymbol{\Psi}_1(x,y) = \boldsymbol{e}_1^-(x, y-d_1)\boldsymbol{a}_1 + \boldsymbol{e}_1^+(x, y-d_1)\bar{\bar{\boldsymbol{R}}}_{12}\boldsymbol{a}_1 \qquad (y \ge d_1) \tag{7}$$

$$\boldsymbol{\Psi}_2(x,y) = \boldsymbol{e}_2^-(x, y)\boldsymbol{a}_2 + \boldsymbol{e}_2^+(x, y)\bar{\bar{\boldsymbol{R}}}_{23}\boldsymbol{a}_2 \qquad (0 < y \le d_1) \tag{8}$$

$$\boldsymbol{\Psi}_3(x,y) = \boldsymbol{e}_2^-(x, y+d_2)\boldsymbol{a}_3 + \boldsymbol{e}_2^+(x, y+d_2)\boldsymbol{R}_{34}\boldsymbol{a}_3 \qquad (-d_2 \le y < 0) \tag{9}$$

$$\boldsymbol{\Psi}_4(x,y) = \boldsymbol{e}_1^-(x, y+d_2)\boldsymbol{a}_4 \qquad (y \le -d_2) \tag{10}$$

with

$$\boldsymbol{e}_1^\pm(x,y) = [e^{ik_{xl}x \pm i\gamma_l y}\delta_{lm}], \quad \boldsymbol{e}_2^\pm(x,y) = [e^{ik_{xl}x \pm i\kappa_l y}\delta_{lm}] \tag{11}$$

$$\boldsymbol{a}_1 = [0 \cdots 0\ 1\ 0 \cdots 0]^t, \quad \gamma_l = \sqrt{k_0^2 - k_{xl}^2}, \quad \kappa_l = \sqrt{k_s^2 - k_{xl}^2} \tag{12}$$

where $k_s = \omega\sqrt{\varepsilon_s \mu_s}$, $\boldsymbol{a}_1$ is the amplitude vector for the downgoing incident waves at $y = d_1$, and $\boldsymbol{a}_2$, $\boldsymbol{a}_3$, and $\boldsymbol{a}_4$ are those of the downgoing space-harmonics defined at the respective reference planes. In Eqs.(8)-(10), $\bar{\bar{\boldsymbol{R}}}_{12}$ and $\bar{\bar{\boldsymbol{R}}}_{23}$ are the generalized reflection matrices connecting the amplitudes of upgoing space-harmonics to those of downgoing ones at $y = d_1$ and $y = 0$, respectively. By tracing the propagation of each space-harmonic in region 1 to region 4, the recursive relations for the generalized reflection matrices $\bar{\bar{\boldsymbol{R}}}_{12}$ and $\bar{\bar{\boldsymbol{R}}}_{23}$ are derived as follows:

$$\bar{\bar{\boldsymbol{R}}}_{12} = \boldsymbol{R}_{12} + \boldsymbol{F}_{21}\boldsymbol{D}_1\bar{\bar{\boldsymbol{R}}}_{23}\boldsymbol{S}_2^{-1}\boldsymbol{D}_1\boldsymbol{F}_{12}, \quad \bar{\bar{\boldsymbol{R}}}_{23} = \boldsymbol{R}^+ + \boldsymbol{F}^-\boldsymbol{D}_2\boldsymbol{R}_{34}\boldsymbol{S}_3^{-1}\boldsymbol{D}_2\boldsymbol{F}^+ \tag{13}$$

with

$$\boldsymbol{S}_2 = \boldsymbol{I} - \boldsymbol{D}_1\boldsymbol{R}_{21}\boldsymbol{D}_1\bar{\bar{\boldsymbol{R}}}_{23}, \quad \boldsymbol{S}_3 = \boldsymbol{I} - \boldsymbol{D}_2\boldsymbol{R}^-\boldsymbol{D}_2\boldsymbol{R}_{34} \tag{14}$$

$$\boldsymbol{D}_1 = [e^{i\kappa_l d_1}\delta_{ln}], \quad \boldsymbol{D}_2 = [e^{i\kappa_l d_2}\delta_{ln}] \tag{15}$$

where $\boldsymbol{R}_{ij}$ and $\boldsymbol{F}_{ij}$ are the diagonal matrices whose elements are given by the Fresnel reflection and transimission coefficients for each of space-harmonics incident from region i toward region j, and $\boldsymbol{R}^{\pm}$ and $\boldsymbol{F}^{\pm}$ are definied by Eq.(1). In the same manner, a recursive relation for the amplitude vectors $\boldsymbol{a}_1$ to $\boldsymbol{a}_4$ is obtained as follows:

$$\boldsymbol{a}_2 = \boldsymbol{S}_2^{-1}\boldsymbol{D}_1\boldsymbol{F}_{12}\boldsymbol{a}_1, \quad \boldsymbol{a}_3 = \boldsymbol{S}_3^{-1}\boldsymbol{D}_2\boldsymbol{F}^{+}\boldsymbol{a}_2, \quad \boldsymbol{a}_4 = \boldsymbol{F}_{34}\boldsymbol{a}_3. \tag{16}$$

These equations lead to the following relation between $\boldsymbol{a}_4$ and $\boldsymbol{a}_1$:

$$\boldsymbol{a}_4 = \bar{\bar{\boldsymbol{F}}}_{14}\boldsymbol{a}_1, \quad \bar{\bar{\boldsymbol{F}}}_{14} = \boldsymbol{F}_{34}\boldsymbol{S}_3^{-1}\boldsymbol{D}_2\boldsymbol{F}^{+}\boldsymbol{S}_2^{-1}\boldsymbol{D}_1\boldsymbol{F}_{12} \tag{17}$$

where the matrix $\bar{\bar{\boldsymbol{F}}}_{14}$ is a generalized transmission matrix for the embedded periodic array of cylindrical objects. The set of Eqs.(13) and (14) is solved recursively by substituing $\boldsymbol{R}_{34}$ to obtain $\boldsymbol{S}_3$, $\bar{\bar{\boldsymbol{R}}}_{23}$, $\boldsymbol{S}_2$ and hence $\bar{\bar{\boldsymbol{R}}}_{12}$. The results are substituted into Eq.(17) to calculate $\bar{\bar{\boldsymbol{F}}}_{14}$.

3. NUMERICAL EXAMPLES

The proposed approach has been applied to the analysis of the array of circular cylinders emdedded in a dielectric slab as shown in Fig. 1. The numerical examples in what follows were obtained by taking into account of the lowest seven space-harmonics and truncating the cylindrical harmonic expansion at $m = \pm 10$ to calculate the T-matrix of the circular cylinder. We discuss here the reflection characteristics for the wavelength range $h/\lambda_0 < 1$ and for the normal incidence with $\phi_0 = 90°$, because such a situation is essential to the use of periodic arrays as the frequency or polarization selective components. In this case, only the fundamental space-harmonic becomes propagating wave outside the dielectric slab. Figure 2 shows the power reflection coefficients R_0 of the fundamental space-harmonic as functions of the normalized wavelength h/λ_0 for the embedded array of circular dielectric cylinders, where $\varepsilon_g/\varepsilon_0 = 2.0$, $\varepsilon_{sl}/\varepsilon_0 = 1.5$, $a = 0.3h$, and $d_1 = d_2 = 0.5h$. The reflection characteristics are drastically changed from those of the free-standing array. There appear two very sharp resonance peaks with supressed side-band reflectance. This is due to the multiple scattering effects between the array and the slab boundaries. Figure 3 shows the simlar plots for the embedded array of perfectly conducting cylinders, where $|\varepsilon_g| = \infty$, $\varepsilon_{sl}/\varepsilon_0 = 3.4$, $a = 0.3h$, and $d_1 = d_2 = 0.5h$. For this case, the lowest three space-harmonics become the propagating waves inside the dielectric slab. It is seen that a complete reflection is attained for both TM and TE waves at different frequency bands. The last example is the embedded array of ferrite cylinders magnetized in the axial direction. For the two dimensional problem, the ferrite cylinder may be treated as a dielectric one with the permittivity ε_g and permeability $\mu_g = \mu_0[(1+\Omega_H)^2 - \Omega_H^2\Omega^2]/[\Omega_H(1+\Omega_H) - \Omega_H^2\Omega^2]$ for TM wave and $\mu_g = \mu_0$ for TE wave, where $\Omega = \omega/\omega_L$, $\Omega_H = \omega_L/\omega_M$, ω_L is the Larmor precession frequecy, and ω_M is the characteristic frequency denoting the saturation magnetization. Figure 4 shows the power reflection coefficients of the embedded ferrite cylinders. The TM wave exhibits a very interesting frequency response. There appear very sharp resonant transimissions at several frequencies, otherwise the incident wave is completely reflected over a wide frequency range. Before concluding, it is worth emphasizing that the errors in energy conservation of the present analyses were less than 10^{-8}.

4. CONCLUDING REMARKS

We have presented a method to calculate the reflected field from a periodic array of cylindrical objects embedded in a dielectric slab. The approach uses the reflection and transmission matrices obtained for the array in free space and the recursive algorithm of the generalized reflection matrix for the multilayered structure. The reflection and transmission matrices of the array can be efficiently calculated using the lattice sums and the T-matrix or aggregate T-matrix of cylindrical objects situated within a unit cell. This is an advantage of the present formulation. The formula (13) can be applied to the embedded multilayered-array problem by replacing $\bar{\bar{\boldsymbol{R}}}_{23}$ by the generalized reflection matrix of the multilayered arrays [7] in free space.

REFERENCES

[1] A. Scherer, T. Doll, E. Yablonovitch, H.O. Everitt, and J.A. Higgins, ed., "Mini-Special Issue on Electromagnetic Crystal Structures, Design, Synthesis, and Applications," IEEE Trans. Microwave Theory Tech., Vol.47, pp.2057-2150, 1999.

[2] J. Y. Suratteau, M. Cadilhac, and R. Petit, "The Perfectly Conducting Wire Grating: Computation of the Diffracted Field from Maxwell's Equations and Hamilton's Canonical System," IEEE Trans. Antennas Propagat., Vol.AP-33, No.4, pp.404-408, April 1985.
[3] H. Roussel, W. C. Chew, F. Jouvie, and W. Tabbara, "Electromagnetic Scattering from Dielectric and Magnetic Gratings of Fibers - a T-matrix Solution," J. of Electromagn. Waves and Appl., Vol.10, No.1, pp.109-127, January 1996.
[4] H. C. Chu, S. K. Jeng, and C. H. Chen, "Reflection and Transmission Characteristics of Lossy Periodic Composite Structures," IEEE Trans. Antennas Propagat., Vol.44, No.3, pp.580-587, March 1996.
[5] K. Yasumoto and K. Yoshitomi, "Efficient Calculation of Lattice Sums for Free-Space Periodic Green's Function," IEEE Trans. Antennas Propagat., Vol.47, No.6, pp.1050-1055, June 1999.
[6] T. Kushta and K. Yasumoto, "Electromagnetic Scattering from Periodic Arrays of Two Circular Cylinders per Unit Cell," to be published in J. Electromagn. Waves and Appl..
[7] K. Yasumoto and T. Kushta, "Electromagnetic Scattering from Multilayered Periodic Arrays of Cylindrical Objects," to be published in the Proc. of CJMW, April 2000.

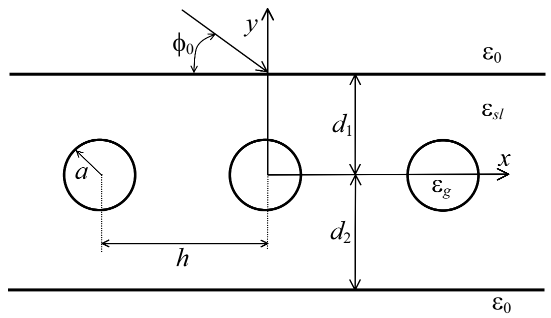

Fig.1 Periodic array of circular cylinders embedded in a dielectric slab.

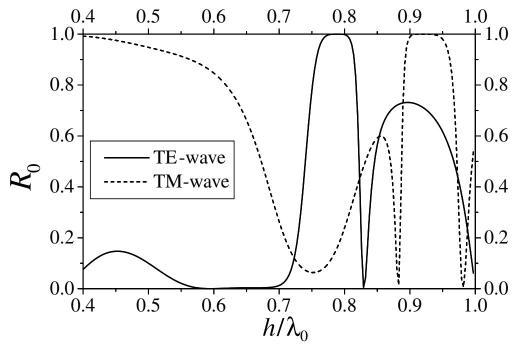

Fig.2 Power reflection coefficient R_0 of the fundamental space harmonic with $l = 0$ for the embedded periodic array of perfectly conducting cylinders as functions of the normalized wavelength h/λ_0 with $\phi_0 = 90°$, $|\varepsilon_g| = \infty$, $\varepsilon_{sl}/\varepsilon_0 = 3.4$, $a = 0.3\,h$, and $d_1 = d_2 = 0.5\,h$.

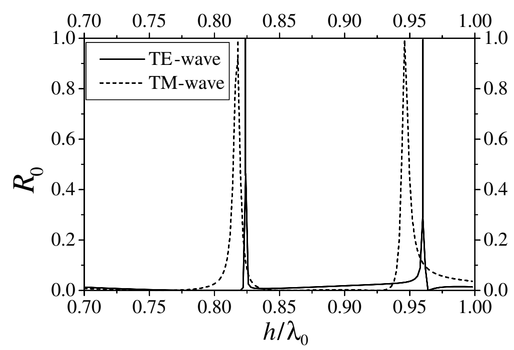

Fig.3 Power reflection coefficient R_0 of the fundamental space harmonic with $l = 0$ for the embedded periodic array of dielectric cylinders as functions of the normalized wavelength h/λ_0 with $\phi_0 = 90°$, $\varepsilon_g/\varepsilon_0$, $\varepsilon_{sl}/\varepsilon_0 = 1.5$, $a = 0.3\,h$, and $d_1 = d_2 = 0.5\,h$.

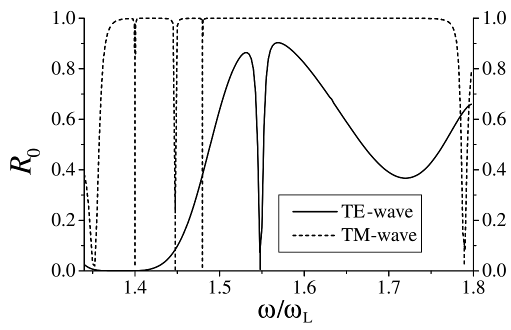

Fig.4 Power reflection coefficient R_0 of the fundamental space harmonic with $l = 0$ for the embedded periodic array of ferrite cylinders magnetized along its axis as functions of the normalized frequency ω/ω_L with $\phi_0 = 90°$, $\Omega_H = 1.3$, $\varepsilon_g/\varepsilon_0 = 14.0$, $\varepsilon_{sl}/\varepsilon_0 = 1.5$, $a = 0.2\,\lambda$, $d_1 = d_2 = 0.25\,\lambda$, and $h = 0.5\lambda$ at $\omega = \omega_L$.